C. R. Chimie 18 (2015) 1229–1241

Contents lists available at ScienceDirect

Comptes Rendus Chimie

www.sciencedirect.com

International Symposium on Air & Water Pollution Abatement Catalysis (AWPAC) – Catalysis for renewable energy

Carbon-based catalysts: Synthesis and applications

María Jesús Lázaro *, Sonia Ascaso, Sara Pérez-Rodríguez, Juan Carlos Calderón, María Elena Gálvez, María Jesús Nieto, Rafael Moliner, Alicia Boyano, David Sebastián, Cinthia Alegre, Laura Calvillo, Veronica Celorrio

Instituto de Carboquímica, CSIC, C/Miguel Luesma Castán, nº 4 50.015, Zaragoza, Spain

ARTICLE INFO

Article history:
Received 7 January 2015
Accepted after revision 8 June 2015
Available online 27 October 2015

Keywords:
Novel carbon materials
Carbon supported catalysts
NO_x reduction
Direct alcohol fuel cells
Electroreduction of CO_2

ABSTRACT

This paper summarizes the main results obtained by the Fuel Combustion Group in three applications: (1) carbon-based catalysts for the selective catalytic reduction (SCR) process of NO_x, (2) Pt and Pt–Ru catalysts for direct alcohol fuel cells, (3) carbon-supported catalysts for the electroreduction of CO_2. Concerning the first aspect, low-cost catalysts able to work at lower temperatures have been prepared and compared with commercial catalysts; for the second one, new catalysts for methanol and ethanol electrochemical oxidation exhibiting current densities that are double those of the commercial ones have been developed; as regards the third one, carbon-supported catalysts for the electroreduction of CO_2 based on Fe and Pd were synthesized and tested. Formic acid was obtained as the main product on all Fe/C electrodes.

1. Introduction

Carbon materials have been used as catalysts for many years. Activated carbons have been considered over the last decades for their utilization in several processes involving heterogeneous catalysis, because they have suitable support properties, as inertness toward unwanted reactions, stability under regeneration and reaction conditions, adequate mechanical properties, modifiable surface area, porosity, and physical form, i.e., the possibility of being manufactured in granulates and conglomerates of different sizes and shapes to suit different chemical reactor configurations [1–4].

However, ACs present two important limitations: their narrow microporosity, which makes difficult mass transport processes and the lack of electrical conductivity, which prevents their use as electrocatalysts. In order to overcome these limitations, new synthetic nanostructured carbon materials such as nanotubes, nanofibers, nanocoils, nanohorns and ordered mesoporous carbons have been developed during the last decade, as new catalyst supports that present several advantages versus activated carbon: they have a better pore structure, more uniform characteristics, a reduced number of impurities and a better electronic structure [4]. Thus, a wide field of applications has been deployed for these materials because they possess electrical and thermal conductivity, as well as a mechanical strength and lightness that conventional materials cannot match [2,5].

The Fuel Conversion Research Group of ICB–CSIC has a long track record in the preparation and characterization of carbon materials [6–15]. In a first stage, ACs obtained from low-rank coals were tested as catalysts and catalyst supports in energy-related reactions such as sulfur and nitrogen emissions reduction from coal combustion and gasification. It was shown that the textural properties and,

* Corresponding author.
E-mail address: mlazaro@icb.csic.es (M. Jesús Lázaro).

http://dx.doi.org/10.1016/j.crci.2015.06.006
1631-0748/

in particular, the surface chemistry of these materials, which is controlled by the presence of oxygen groups, were well suited to carry out such reactions.

With the arrival on the scene of renewable energies, in particular renewable electricity, the interest in the conversion energy processes moved toward the electrochemical reactions involved in electrochemical devices such as fuel cells and solar fuels harvesting by means of CO_2 electrochemical reduction. Activated carbons are not adequate for these applications due to their lack of electrical conductivity and their narrow microporosity, so new carbon materials intended to overcome these limitations were synthesized: carbon nanofibers (CNF), nanocoils (CNC), and xerogels (CXG), as well as ordered mesoporous carbon materials (OMC) and carbon blacks (CB), e.g., the commercial material Vulcan XC-72R, have been synthesized and used as catalytic supports for different applications [6–39]. Carbon materials have been obtained using different methods. In the case of carbon nanofibers, they were synthesized by methane decomposition on a $NiCuAl_2O_3$ catalyst. This catalyst was prepared by co-precipitation of the metal nitrates, followed by a calcination process at 450 °C. Later, a methane flow is passed through a furnace containing the catalyst at 700 °C for 10 h, transforming this molecule into molecular hydrogen and carbon deposited in nanofiber shape. On the other hand, carbon nanocoils were synthesized by the catalytic graphitization of a resorcinol–formaldehyde gel. In this procedure, formaldehyde and silica sol were dissolved in deionized water. Then, nickel and cobalt salts mixtures were added before the addition of resorcinol as an organic precursor. This mixture was heat-treated at 85 °C for 3 h and dried at 108 °C. Finally, it was carbonized in a nitrogen atmosphere at 900 °C for 3 h. Removal of silica particles was achieved by a chemical treatment with a concentrated NaOH solution, followed by a treatment with concentrated HNO_3. For the synthesis of carbon xerogels, resorcinol, water, formaldehyde and sodium carbonate were mixed under stirring in ratios that promote the obtaining of highly porous xerogels. The mixture was put into closed vials and cured for 24 h at room temperature. After that, the vials were heated in an oven at 50 °C for 24 h and dried at 85 °C for 120 h. The pyrolysis of the organic gels was performed at 800 °C during 3 h under an N_2 flow. Finally, ordered mesoporous carbons were obtained by incipient wetness impregnation method using ordered mesoporous silica as a template and a furan resin/acetone resin as a carbon precursor. Silica was impregnated with the carbon precursor and after carbonized at 700 °C for 2 h. Subsequently, the silica–carbon composite was washed with NaOH in ethanol to remove the silica. Further details can be found elsewhere [6–15]. From these works, carbons with different physicochemical properties have been obtained. Thus, CNF and CNC show a crystalline structure with well-aligned graphene layers, while OMCs exhibit a hexagonal ordered structure composed of amorphous carbon. In contrast, CXG are mainly composed of non-crystalline carbon aggregates, which are characterized by the random aggregation of primary carbon spheres. All these materials present different textural properties, with a surface area increasing in the order CNF < CB < CNC < CXG < OMC, covering a wide interval of values from 70 $m^2 \cdot g^{-1}$ for carbon nanofilaments, due to their lack of microporosity, to 1050 $m^2 \cdot g^{-1}$ for OMC. This last material presents a very developed surface area, which is associated with their porous structure based on periodic carbon cylinders, with uniform mesopores between them.

Although the activated carbons and the mesoporous carbons described above present very different textural properties, their surface chemistry present many similarities because each of them is controlled by the presence of oxygen groups. As a consequence, their acid–base and redox properties and therefore their performances as a catalyst can be studied with analogous physicochemical criteria.

In this summary of the keynote presented at the AWPAC 2014 (3rd International Symposium on Air & Water Pollution Abatement Catalysis), the results obtained in three different applications related to the topics of the conference are presented:

- carbon-based catalysts for the selective catalytic reduction of NO;
- Pt and Pt–Ru catalysts for direct alcohol fuel cells;
- carbon-supported catalysts for CO_2 electroreduction.

2. Carbon-based catalysts for the selective catalytic reduction of NO

Nitrogen oxides, NO_x, have a huge impact on our environment. They generate acid rain, soil eutrophication and acidification, as well as water nitrification, and also they contribute to ozone formation in the lower layers of the atmosphere. They are generated in every combustion process making use of a fossil or N-containing fuel and/or, most importantly, when combustion takes place under air atmosphere at high temperatures (> 900 °C). Increasingly stricter environmental regulations concerning the emission of nitrogen oxides (NO_x) have forced the development of more efficient technologies to reduce the emission of these pollutants from small and medium industrial facilities. Activated carbons have been used as catalysts in De-NO_x after-treatment technologies. They can act as a NO_x reductant itself [40,41], as a catalyst or as a catalyst support, either in the presence or in the absence of an external reducing agent.

The selective catalytic reduction (SCR) is the reduction of nitrogen oxide in the presence of a catalyst and a reducing agent. The use of carbon-based catalysts in this process has been studied in the last years, because they are able to bring down the optimal reaction temperature for achieving high De-NO_x conversions in comparison to TiO_2-based catalytic systems. Several carbon materials have been impregnated with Cu [42,43], Fe [42], Mn [44–46] and V compounds [20,21,47].

Catalysts containing vanadium as active metal supported on activated carbons were extensively studied by Lázaro et al., investigating as well the use of petroleum coke ashes as a V-source [21]. The authors optimized [22] the features of the activated carbon support, modifying several parameters in the preparation process via steam activation of a low-rank coal. They observed that adequate

surface area, porosity and oxygen surface groups (mainly basic groups, such as phenolic) were necessary because of their decisive role in vanadium fixation on the carbon surface, even more when petroleum coke ashes were used as the active phase precursor. Fig. 1 shows the NO reduction measured in the selective catalytic reduction (SCR) reaction, in the presence of ammonia and O_2 at 150 °C using several catalysts synthesised with different activated carbon supports and petroleum coke ashes (PCA) as the V-source, corresponding to a 3% wt V-load. The activity was increased for the catalyst supported on the carbon support with the highest amount of surface groups. The functionalization of the supports using HNO_3 pre-treatments yielded higher NO conversions, reaching almost 90% in some cases [20].

The elucidation of the different steps in the mechanism of the SCR of NO over V-loaded activated carbons was studied by Gálvez et al. [23] using temperature-programmed desorption (TPD), ammonia chemisorption, *in situ* DRIFT spectrometry and transient response analysis. Ammonia adsorption on the catalyst's surface was a key step in the overall reaction mechanism because it could be adsorbed in the metallic centres (V) and in the oxygen surface groups (most probably carboxylic acids). The presence of oxygen surface functionalities can be beneficial, as seen in this last example, or detrimental, as observed in the hindered adsorption of phenol on the surface of acidic activated carbons [48,49].

The following step of the study was the briquetting of the catalyst in order to obtain catalysts that present a lower pressure drop [21,24–28]. They produced carbon briquettes from a low-rank coal pyrolized at 800 °C, blended with a commercial tar pitch and cold pressed at 125 MPa. The obtained cylindrical briquettes were then cured in air and pyrolized at 800 °C. After that, the briquettes were activated in the presence of either CO_2 or H_2O and functionalized using HNO_3 and H_2SO_4. Vanadium as an active phase was introduced by impregnation using different precursors, as V obtained from the ashes of a petroleum coke (PCA). The mechanical strength of the catalytic briquettes was evaluated by means of the Impact Resistance Index (IRI) and the Water Resistance Index (WRI), following the procedure described by Richards [50]. The activation process notably influenced the mechanical properties of the carbon briquettes. IRI increased after activation either with steam or CO_2, with respect to the pyrolized briquette. The activation of the briquettes led to a decrease in the mechanical strength, similar to that reported by Rubio et al. [51] and Amaya et al. [52]. WRI was mostly affected by the chemistry of the briquettes. According to the mechanism postulated by Ozaki et al. [53], carboxylic groups avoid the adsorption of water on the external surface of the briquette, which retards the formation of cracks and their propagation.

Fig. 2 shows the activity of catalytic briquettes. The activity depends on the surface area and the amount of basic oxygen surface functionalities on its surface. An adequate development of porosity was necessary to avoid pore blockage, especially after the deposition of the active phase, favouring the diffusion of reactants and products out of the structure of the briquette. The presence of surface functionalities promoted support-active phase interaction resulting in enhanced catalytic activity [28].

The next step was to prepare the catalyst as carbon-coated cordierite monoliths [29,30] using furan resin and polyethylene glycol, which was carbonized and activated with CO_2 at 800 °C. They reported that the resin yielded the carbon layer during pyrolysis, whereas polyethylene glycol helped in the creation of mesopores. On the other hand, activation with CO_2 contributed to the formation of new micropores. Upon vanadium addition, by means of an equilibrium adsorption using ammonium metavanadate as a precursor, they observed that oxygen surface functionalities were decisive for an optimal distribution of the active phase. Up to 6% wt. of vanadium loading, the catalysts showed activities comparable to that of similar SCR catalytic systems reported in the literature, with complete selectivity towards N_2. An increasing vanadium content resulted in less uniform distributions of the active phase. By simulating the influence of the coating thickness on the geometric parameters and conversion, they identified and optimal coating thickness around 30 μm reaching

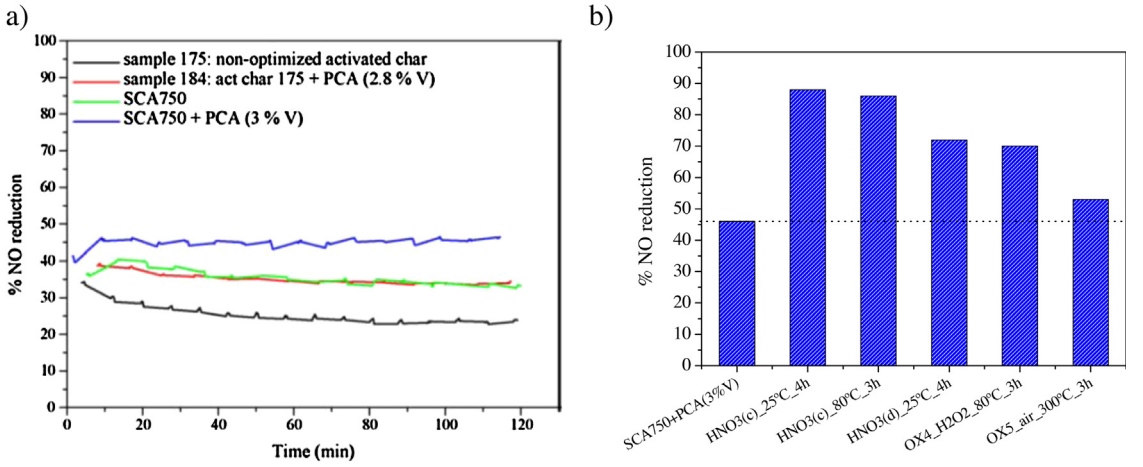

Fig. 1. (Colour online.) Nitrogen oxides (NO) reduction at 150 °C in the presence of NH_3 and O_2 measured for: a: a series of V-loaded activated carbons; b: catalysts prepared using pre-oxidized carbon supports.

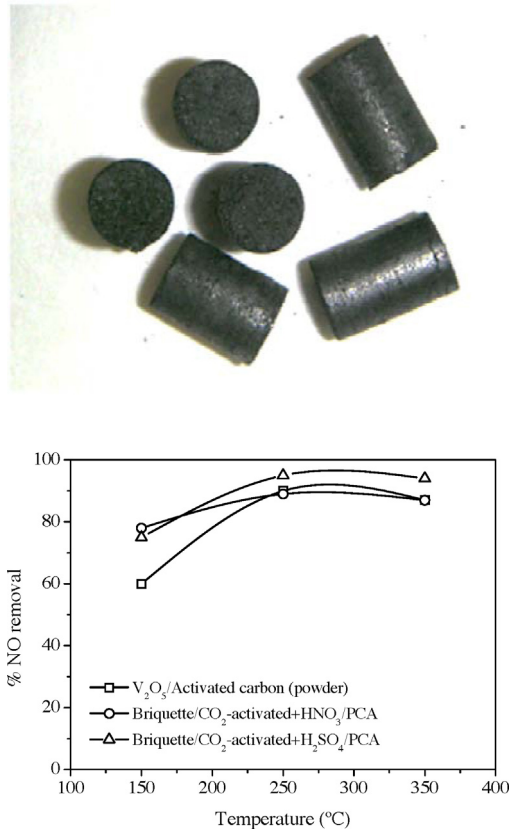

Fig. 2. (Colour online.) Nitrogen oxides (NO) removal as a function of temperature.

a compromise between activity and pressure drop. The influence of oxidation pre-treatments on carbon-coated honeycomb monoliths was also studied by the same authors [31], as well as their catalytic behaviour in the SCR of NO in the presence of steam and SO_2 (see Fig. 3)

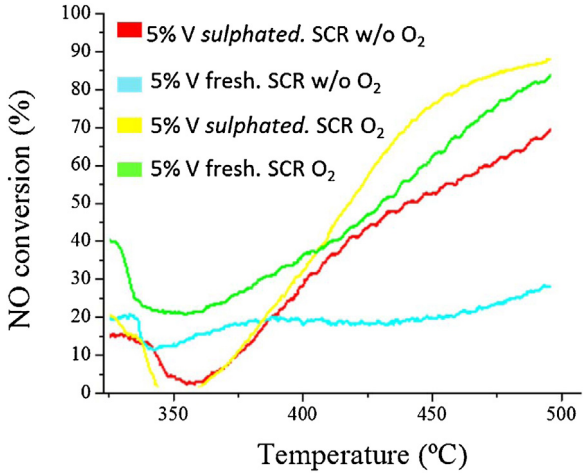

Fig. 3. (Colour online.) Nitrogen oxides (NO) conversion for V-loaded carbon monoliths, be they fresh or submitted to a pre-oxidation treatment using H_2SO_4; in the presence of 500 ppm of NO, 600 ppm of NH_3, 3% of O_2 (when added).

[32]. Using several characterization techniques, such as Fourier transform infrared spectroscopy, X-ray photoelectron spectroscopy and temperature-programmed desorption, they concluded that pre-treatment of the carbon-coated monoliths at 330 °C in the presence of 10% of O_2–Ar induces the formation of an optimal amount of surface groups resulting in the highest vanadium loading at high dispersion. Vanadium loading depends not only on the amount of oxygen-containing groups, but also on the textural properties of the carbon. At temperatures higher than 200 °C, the vanadia-loaded carbon-coated monoliths were able to maintain their activity in the SCR of NO in the presence of steam and SO_2, due to an auto-regenerating mechanism in which ammonium sulphate salts were instantaneously decomposed as long as they were formed and deposited on the catalyst's surface.

3. Pt and Pt–Ru catalysts for direct alcohol fuel cells

The use of renewable energy sources has captured the attention of scientists, in order to find solutions for "green-energy" generation, avoiding the production of pollutants from the use of petroleum fuels. Polymer electrolyte membrane fuel cells are a technology able to take part in renewable energy sources, because they convert chemical energy into electric power, by means of the oxidation of a continuously supplied fuel [54], clean-produced, noiseless and efficient electric energy [55] for mobile, stationary, and portable applications.

Direct methanol fuel cells (DMFC) are a subcategory of PEM fuel cells, which use methanol as a fuel. Some of the advantages of methanol use are its easy storage, higher energy in a small volume unit, less polluting reaction products and long operation times. Nevertheless, DMFCs present two main technological disadvantages:

- the passage of methanol through the membrane or *crossover* [56,57], diminishing the cell potential due to its oxidation on the cathode;
- the poisoning of the anode with carbon monoxide, which is strongly adsorbed on Pt surface [57–59], reducing the catalytic surface area and the cell performance.

In this sense, the design of Pt-carbon-based catalysts with novel properties is an interesting research subject due to the necessity of overcoming these troubles, and also to reduce the production costs of their components. Recently, several investigations have been focused on the use of different Pt alloys with transition metals [60–63] and the use of novel carbon supports.

Concerning carbon supports, it has been reported that the use of novel synthetic carbon materials with a more ordered structure and better surface and electrical properties enhances fuel cell performance. Some of these carbon materials are: graphite nanofibers [64,65], carbon nanotubes [66,67], carbon microspheres [68], hard carbon spherules [69], carbon aerogels and xerogels [70,71], and mesoporous carbons [72,73]. Particularly, carbon nanofibers (CNFs) have become notorious for their suitable textural properties such as surface area, pore volume, and high electrical conductivity. Carbon xerogels also can be

used as carbon supports, taking into account their mesoporous and macroporous textures and large pore volume. These supports possess excellent characteristics, such as high porosity, high surface area, controllable pore size and different forms (monolith, thin film or powder), depending on the desired use [74]. On the other hand, ordered mesoporous carbon structures draw attention because of their applications in catalysis and energy storage. These carbons are synthesized by nano-casting methods, using ordered silica templates [75].

Different carbon materials have been used as supports for Pt and Pt–Ru catalysts, obtaining desirable anode and cathode materials for direct alcohol fuel cells. An optimization of carbon nanofibers, carbon xerogels and graphitized ordered mesoporous carbons has been made in order to determine the influence of the properties of the carbon supports, which affect the performance of the fuel cell.

3.1. Pt and Pt–Ru catalysts supported on carbon nanofibers

The properties of carbon supports (such as surface area, pore volume, electrical and thermal conductivity, corrosion resistance) strongly influence the properties of the catalysts (activity, transport of electrons, heat dissipation, and stability in time) [5]. In the case of carbon nanofibers, these characteristics principally depend on the structure generated with graphite plane stacks [76], which can be modified by reaction temperature, gas composition, and the nature of the catalyst employed during the growth of carbon nanofibers [5,33,77–79]. Sebastián et al. [34] reported that an increase in the growth temperature of carbon nanofibers from 550 to 700 °C induces a decrease in the catalytic activity of Pt nanoparticles supported on this carbon material towards the electrochemical oxidations of both CO and methanol in acid media (0.5 M H_2SO_4).

Fig. 4 [34] shows that the catalyst supported on the grown-up carbon nanofiber at the lowest temperature (550 °C) displayed the highest electrochemical activity in comparison with those prepared at higher temperatures. In the case of the stripping of a CO monolayer adsorbed at 0.20 V vs. RHE, two CO oxidation peaks were observed, the first one close to 0.73 V and the second one near to 0.83 V; the second peak shifts to more positive potentials with an increase in the temperature of carbon nanofiber growth; meanwhile, the Pt/C commercial catalyst developed a single CO oxidation peak occurring at 0.86 V. The catalyst supported on the nanofiber synthesized at 550 °C has the biggest amount on surface groups [34], which promote the electronic transference by means of these groups and benefit to CO oxidation at lower potentials. This fact was also evident in methanol electrochemical oxidation, which again displayed the best behavior for the Pt catalysts supported on carbon nanofibers prepared at 550 °C.

Pt–Ru alloys are recognized as good catalysts for carrying out the electrochemical oxidation of low-weight alcohols, because of the generation of OH_{ads} at low potentials, which are able to promote the oxidation of the formed carbon monoxide as intermediates in the oxidation reaction of alcohol [58]. Nanoparticles of this alloy have been supported on carbon nanofibers synthesized at different growth temperatures in order to determine their catalytic activity towards the oxidation

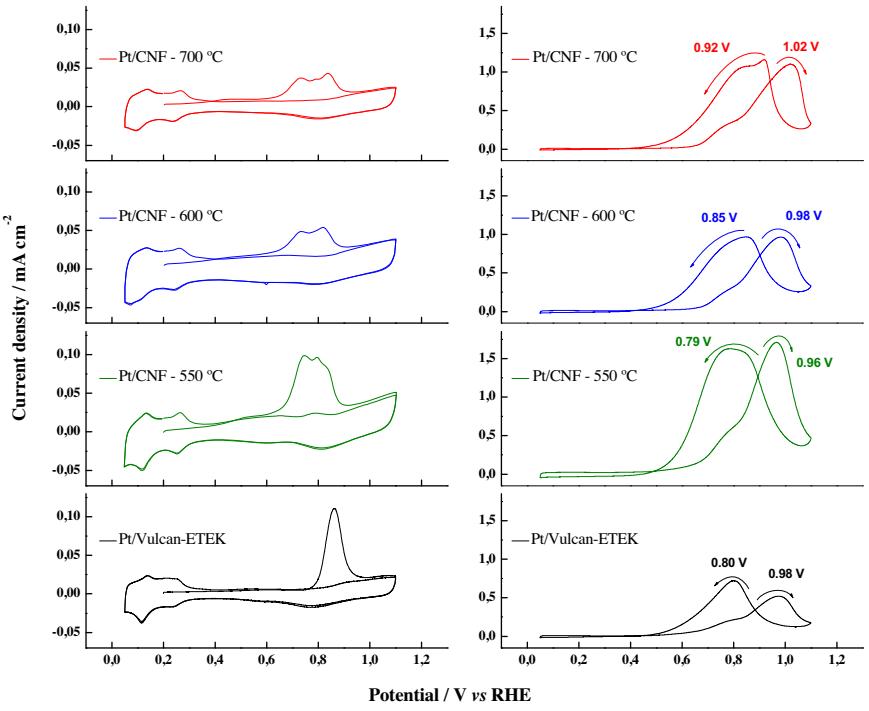

Fig. 4. (Colour online.) Activity of Pt nanoparticles supported on carbon nanofibers grown at different temperatures, in acid media. Left side: CO stripping adsorbed at 0.2 V vs. RHE. Right side: electrochemical oxidation of methanol; RHE: reference hydrogen electrode; CV: cyclic voltammograms; MSCV: mass spectrometric cyclic voltammograms.

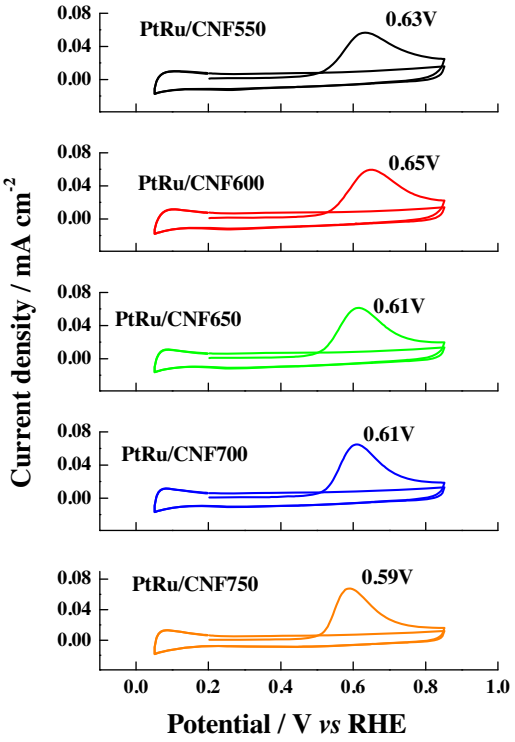

Fig. 5. (Colour online.) CO electrochemical oxidation on Pt–Ru catalysts supported on carbon nanofibers synthesized at different temperatures. Scan rate: 20 mV·s^{-1}. Supporting electrolyte: 0.5 M H_2SO_4. CO adsorption potential: 0.2 V vs. RHE.

of methanol and ethanol at room temperature, leading to a relation between carbon nanofiber crystallinity, pore volumes, and electrocatalytic activity [8]. Fig. 5 shows the cyclic voltammograms of CO oxidation, when this molecule is adsorbed at 0.2 V vs. RHE in acid media (0.5 M H_2SO_4); a single peak was observed in the range from 0.59 to 0.65 V, and no double peaks or pre-peaks were seen, as in the case of Pt/CNF catalysts. The differences among the materials were explained in terms of the CO oxidation peak potentials and their correlation with the graphitization degree of the support; again, the authors suggest that the amount of graphitic planes affects the metal–support interaction, favoring CO electro-oxidation at more negative potential values, although the similarity of the peak potential values was also attributed to the regular growth of the nanoparticles inside micelles, bearing in mind the fact that the catalysts were synthesized by a microemulsion method. On the other hand, it was found that methanol oxidation currents are enhanced with the increase of the graphitization degree of carbon nanofibers (see Fig. 6), a fact attributed to a major metal–support interaction; nevertheless, an excessive increase of graphicity, and thus, a decrease in the pore volume of the carbon support and oxygen functional groups, as that obtained at 700 °C and 750 °C during the carbon nanofibers synthesis process, decreased the activities of the catalysts towards the electrochemical oxidation of ethanol (Fig. 7); ethanol oxidation current densities lower than those for the methanol were observed, this result being coherent with both, the slower kinetics for ethanol oxidation and the influence of the carbon nanofibers properties, bearing in mind the decrease in the pore volumes of the different graphitized carbon nanofibers, when the temperature is increased. This fact suggested that ethanol diffusion through the carbon nanofiber structure controls the kinetic of ethanol oxidation, considering that in materials with low pore volumes, as in the case of the highly graphitized carbon nanofibers, oxidation current densities were low and thus, catalytic activity diminished.

3.2. Pt and Pt–Ru catalysts supported on carbon xerogels

Carbon xerogels are another type of carbon support intensively studied in the last few years, because of their

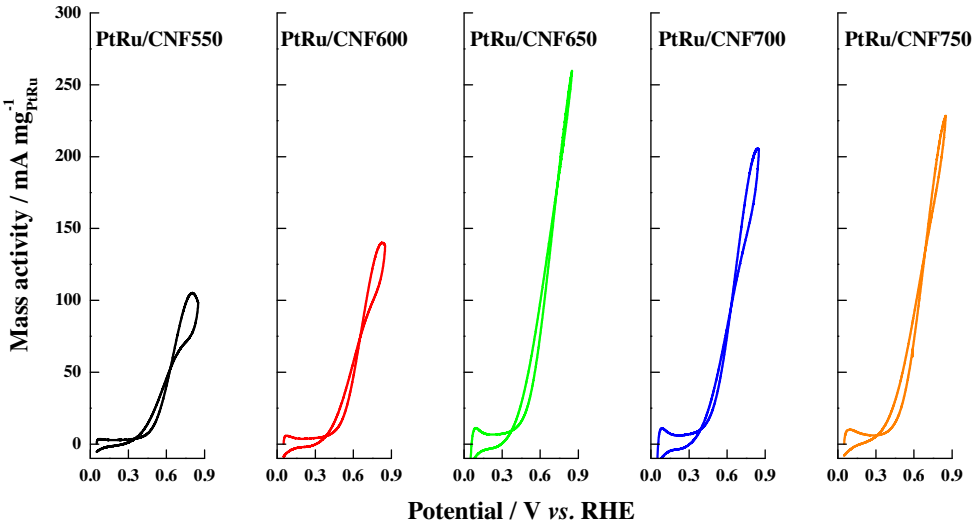

Fig. 6. (Colour online.) Methanol electrochemical oxidation on Pt–Ru catalysts supported on carbon nanofibers synthesized at different temperatures. Scan rate: 20 mV·s^{-1}. Supporting electrolyte: 0.5 M H_2SO_4. Methanol concentration: 2.0 M.

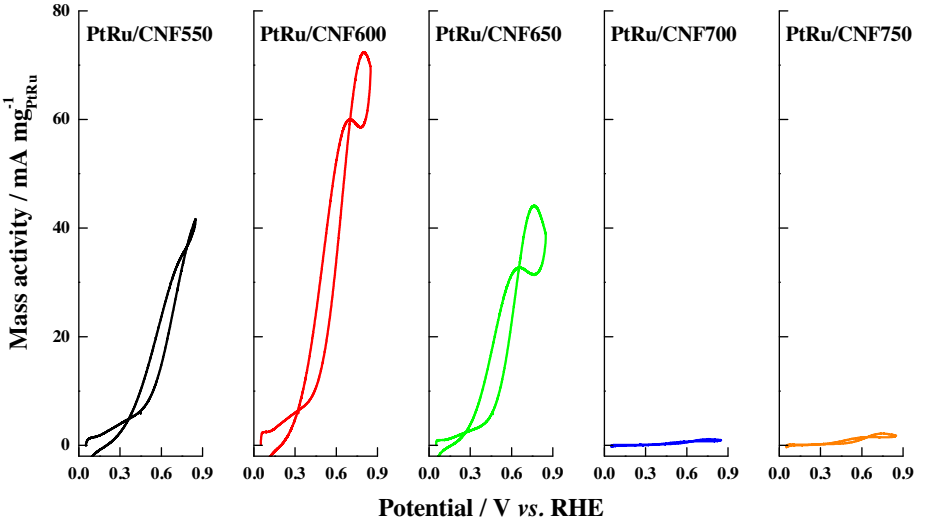

Fig. 7. (Colour online.) Ethanol electrochemical oxidation on Pt–Ru catalysts supported on carbon nanofibers synthesized at different temperatures. Scan rate: 20 mV·s^{-1}. Supporting electrolyte: 0.5 M H_2SO_4. Ethanol concentration: 2.0 M.

interesting properties as high surface area, rich and interconnected mesopore structure and modifiable pore-size distribution [80–82]. Alegre et al. [15] prepared Pt catalysts supported on a carbon xerogel employing sodium borohydride (SBM), formic acid (FAM), and a microemulsion as synthesis methods, in order to study their activity towards the oxygen reduction reaction when they are employed as cathodes in a direct methanol fuel monocell operating at 60 °C. These routes allow obtaining catalysts with different properties: FAM-reduced catalysts displayed the highest performance and activity in both, polarization and power density curves (Fig. 8a), whereas the comparison with the Pt catalyst supported on Vulcan carbon black and prepared using the same methodology also exhibited enhanced activity, as shown in Fig. 8b. These facts were explained by the obtaining of a low crystallite size (3.6 nm) for the FAM-synthesized material in comparison with the values determined in the case of the catalysts prepared by the borohydride and microemulsion routes (4.2 nm and 3.9 nm, respectively). Moreover, Pt/CXG-FAM presented a slightly major performance than that for the catalysts supported on the commercial Vulcan carbon black Pt/CB FAM, prepared by the same synthesis route, suggesting that the resistance of the catalysts supported on carbon xerogel is comparable with that of carbon black, in spite of its lack of graphitic planes, which are present in the commercial carbon material.

Alegre et al. [35] synthesized Pt–Ru catalysts supported on carbon xerogels using different synthesis routes to evaluate the catalytic activity towards the CO and methanol electrochemical oxidation. The results for the first reaction appear in Fig. 9a and the higher tolerance towards CO poisoning was detected for the PtRu/CXG-ME catalyst, which was prepared by the microemulsion route, generating the most negative CO oxidation peak potential.

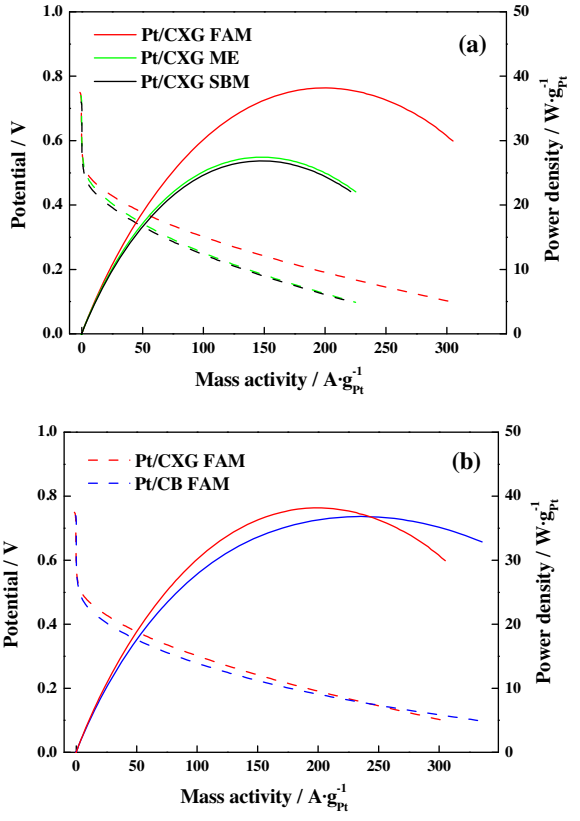

Fig. 8. (Colour online.) a: polarization curves (dashed lines) and power density curves (full lines) for Pt/carbon xerogels (CXG) catalysts, synthesized by different synthesis methods; b: comparison between Pt catalysts supported on carbon xerogel (red line) and carbon black (blue line); in this case, both catalysts were reduced by formic acid reduction [formic acid (FAM) method].

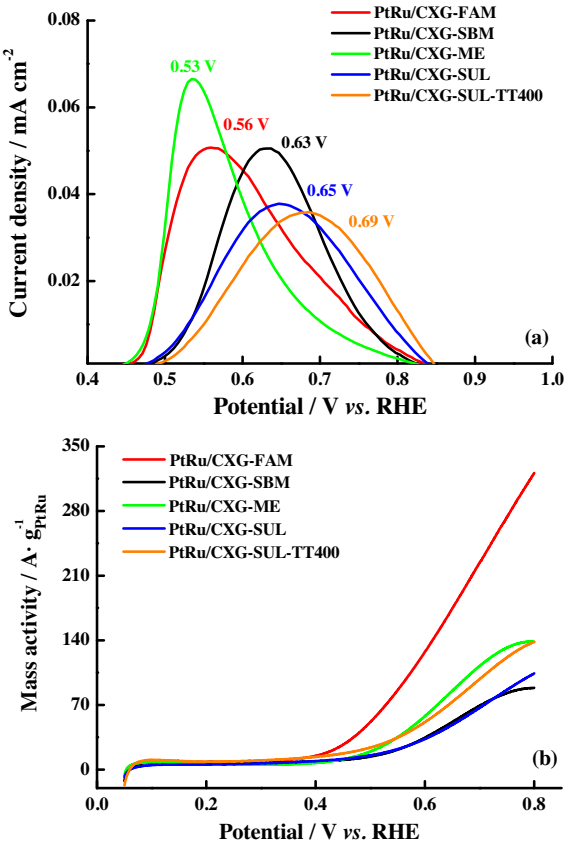

Fig. 9. (Colour online.) a: CO stripping on the Pt–Ru catalysts supported on carbon xerogels in acid medium; b: methanol electrochemical oxidation on the same catalysts. Scan rate: 20 mV·s^{-1}. Support electrolyte: 0.5 M H_2SO_4. Methanol concentration: 2.0 M. CO adsorption potential: 0.2 V vs. RHE.

This tolerance decrease in the other materials following the next order: the formic acid reduced catalyst (PtRu/CXG-FAM), sodium borohydride (PtRu/CXG-SBM), and those synthesized by a new methodology, the sulfite complex catalysts PtRu/CXG-SUL and PtRu/CXG-SUL-TT400. This order was explained by the high surface Ru content observed for the catalyst synthesized by the microemulsion method, which also present a high alloy degree with Pt, according to the determined lattice parameter. The presence of agglomerates with high content of crystal defects in PtRu/CXG-FAM explained the obtaining of a negative CO oxidation peak potential, whereas the low alloying degree and lower metallic Ru content in SBM catalyst could be the reasons for the more positive CO oxidation peak potential observed for this material. The catalysts prepared by the sulfite complex method displayed the worst activity and it was associated with the lowest particle sizes determined for these materials, which probably suffer from a lack of crystal defects and planes, which are necessary for them to react. On the other hand, the methanol electrochemical oxidation was carried out on these materials, and the results are presented in Fig. 9b; the reactivity order shows the best performance for the PtRu/CXG-FAM catalyst, possibly because of their largest crystal size, high segregation of Pt on the catalyst surface, and better combination of Pt and Ru atoms. PtRu/CXG-SUL-TT400 also presented a high content of Pt at the surface but a low alloy degree with Ru, suggesting a key role for this parameter in the activity towards the methanol electrochemical oxidation.

3.3. Pt and Pt–Ru catalysts supported on graphitized ordered mesoporous carbons

Ordered mesoporous carbons (OMCs) have received great interest in the last few years because of their potential application in different fields such as energy storage, separation, adsorption, and catalysis [83–86]. In order to be employed as electrocatalyst supports, these carbonaceous materials must have tunable textural properties and surface chemistry, besides regular structure, high surface area, large pore volume, narrow pore-size distribution and high electrical conductivity [87]. Calvillo et al. [36] reported the graphitization of CMK-3 ordered mesoporous carbon, in order to increase its conductivity and thus, the activity of catalysts towards the CO and methanol electrochemical oxidation. Graphitization of OMCs was achieved by a heat treatment of the carbon material at 1500 °C. Fig. 10 displayed the results for CO stripping on the catalysts supported on graphitized OMCs and the comparison with the signal observed for the commercial catalyst Pt/C E-TEK. In both cases, only one CO oxidation peak was observed, although the value for Pt/gCMK-3 was located at more negative potential values than the ones observed for commercial catalysts (0.79 V compared with 0.84, respectively), indicating an increase in catalytic activity attributed to the enhancement of the electroactive species diffusion. The methanol and ethanol electrochemical oxidations on

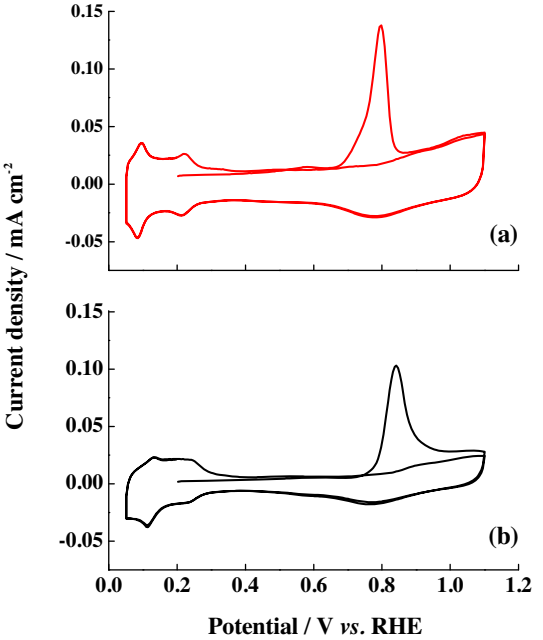

Fig. 10. (Colour online.) CO stripping on (a) Pt/gCMK-3 catalysts and (b) Pt/C E-TEK commercial catalyst. Scan rate: 20 mV·s^{-1}. Support electrolyte: 0.5 M H_2SO_4. CO adsorption potential: 0.2 V vs. RHE.

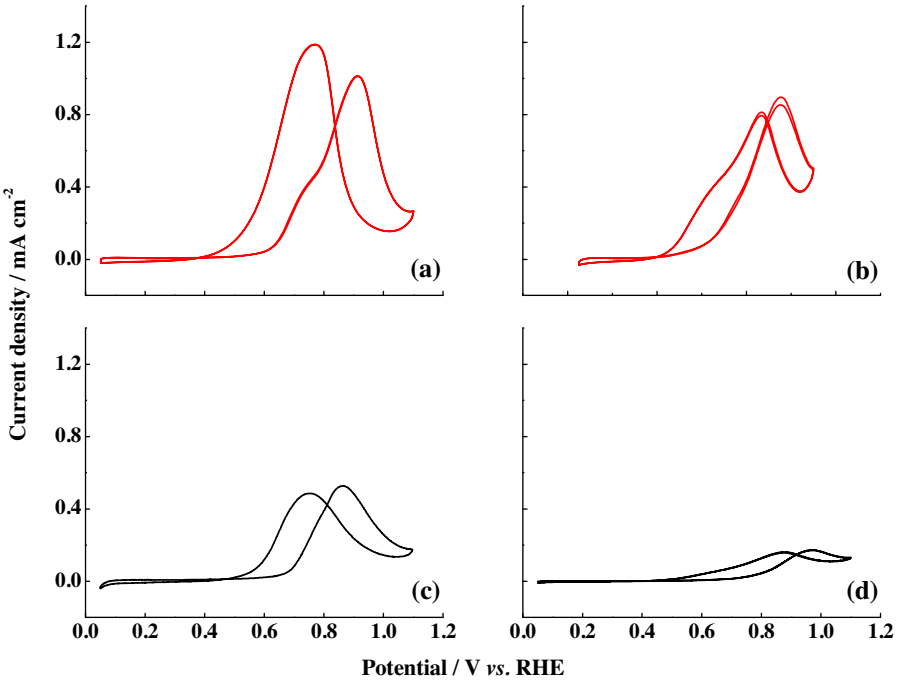

Fig. 11. (Colour online.) Methanol electrochemical oxidation on (a) Pt/gCMK-3 and (b) Pt/C E-TEK, and ethanol electrochemical oxidation on (c) Pt/gCMK-3 and (d) Pt/C E-TEK. Scan rate: 20 mV·s^{-1}. Support electrolyte: 0.5 M H_2SO_4. Methanol and ethanol concentrations: 2.0 M.

this catalyst and the comparison with the commercial catalyst are presented in Fig. 11. In both fuels, the current densities overcome that obtained for the commercial catalyst by a factor of two or even more. This reaction was studied for the catalysts supported on the carbon material without heat treatment [38], but lower current densities were detected, so the enhanced performance of the Pt/gCMK-3 catalyst could be attributed to the high electrical conductivity of the modified gCMK-3 carbon support, generated by heat treatment.

From the results presented in this part of the review, it could be seen that different carbon materials can be used as supports for DMFC catalysts, even though there are several differences between them, with consequences on the activity of the catalysts. These differences in morphology, structure, crystallinity of both carbon support and metal nanoparticles, and surface chemistry affect the electrochemical activity of the catalysts through some properties, as electrochemical conductivity, electronic transferences, increase of active sites, enhancement of metal nanoparticle–carbon support interaction, and the diffusion of electroactive species. The effects of these differences are evidenced by two facts: first, low CO oxidation peak potentials, which represent a high tolerance towards poisoning and, second, high methanol oxidation current densities, and thus explain the high performances of the catalysts when they are used as anodes in direct methanol fuel cells.

4. Carbon-supported catalysts for CO_2 electroreduction

CO_2 emissions caused by the burning of carbon-rich fossil fuels for obtaining electricity and energy have been increasing since the industrial revolution, which may result in serious global warming problems. Consequently, the reduction in global CO_2 emissions is currently a critical issue and several CO_2 mitigation strategies have been developed. Among them, CO_2 conversion to valuable products for energy source or chemical industry has attracted special attention. Chemical, electrochemical, thermochemical, photochemical, and biochemical methods have been proposed for CO_2 conversion. It is well known that the electrochemical route is a possibility for producing a variety of useful products (methane, monoxide carbon, acid formic, methanol, etc.) [88,89].

The electrochemical reduction of CO_2 has been studied for many years using various metallic electrodes since the product distribution strongly depends on the used material [88–91]. Efficient catalysts for CO_2 reduction should provide both CO_2 activation and subsequent hydrogenation into reduced species. For this reason, metals with low hydrogen overpotentials, such as Pt and Pd, have been widely used, since these materials adsorb easily hydrogen, which may interact with intermediates derived from CO_2 activation [18,92–95]. CO_2 is reduced to strongly adsorbed CO on Pt, inhibiting further CO_2 transformation [92]. However, adsorbates from CO_2 reduction may behave as intermediates on Pd, obtaining CO and formic acid as the main products [93,95]. On the other hand, Cu has attracted also special attention, since hydrocarbons, aldehydes and alcohols can be obtained using this metal as a catalyst, generating significant current densities [91]. The use of other group-VIII element metals (such as Fe, Co, Ni) has been also studied due to their low-cost [89,90]. However, these electrodes show low electrocatalytic activity in CO_2 electroreduction in

aqueous solutions and room conditions, with H_2 (formed by water reduction) as the major product.

The mains drawback of this process is the low solubility of CO_2 in water at atmospheric pressure and room temperature. In order to address this limitation, high pressures [96–98], low temperatures [96,99–103], and/or non-aqueous solvents (dimethyl-formamide, methanol, propylene carbonate, acetonitrile) [102–106] have been used. Another important alternative to enhance the rate of the CO_2 reduction reaction is the use of gas diffusion electrodes (GDEs) or metal catalysts based on nanostructured carbon materials [17,18,107–110]. These porous electrodes present a large reaction area while providing low current density. A significantly higher current density and a different product distribution have been found using supported catalysts than when using the corresponding bulk electrode. Furthermore, carbon-based electrodes can favour CO_2 activation, decreasing the overpotential of the reaction. Surprisingly, isopropanol and acetone, together with a mixture of C3-C9 hydrocarbons, were found in a Fe catalyst supported onto carbon nanotubes, while Pt/CNT showed less productivity towards these products, although with a slower deactivation [110]. However, there are not many studies about CO_2 electroreduction on GDEs or carbon-supported catalysts.

The Fuel Conversion Research Group of ICB-CSIC has been working on the use of GDEs or catalysts supported onto carbon materials for the CO_2 valorisation by an electrochemical route [17,18]. Fe and Pd metals have been selected as the active phase of the electrodes. On the other hand, novel nanostructured carbon materials, such as carbon nanofibers (CNF), carbon nanocoils (CNC) and ordered mesoporous carbon (OMC), as well as treated Vulcan XC-72R, have been tested as supports of the electrocatalysts.

4.1. Fe catalysts supported on treated Vulcan XC-72R

Fe electrodes present a low efficiency for CO_2 electroreduction in aqueous solutions and room conditions, being H_2 the main electrolysis product. However, the use of supported catalysts could favor the reaction. Our group has obtained promising results towards the CO_2 reduction reaction using GDE based on iron-oxide catalysts supported on treated Vulcan XC-72R [17].

Fe electrocatalysts with a metal loading of 20 wt. % were prepared by the polyol method, using ethylene glycol as the solvent and the reducing agent. Prior to metal deposition, Vulcan was subjected to different oxidation procedures with concentrated HNO_3 (Nc) or a mixture HNO_3–H_2SO_4 1:1 (v/v) (NS), in order to create functional groups. The treatments were performed at room (T_a) or boiling (T_b) temperatures, during 0.5 or 2 h. GDEs were obtained by deposition of a layer of the corresponding catalyst ink onto a carbon cloth treated thermally [17]. The original material Vulcan and the modified carbon supports as well as the Fe-based catalysts were physicochemically characterized by different analytic techniques (e.g., XRD, TEM, N_2 adsorption and TPD) in order to study the textural and structural properties, the morphology and the surface chemistry of the carbonaceous materials, and the size and dispersion of metal particles. Additionally, the electrochemical properties of the electrodes and the formation of gaseous and volatile products/intermediates of the reduction of CO_2 were followed by *in situ* differential electrochemical mass spectrometry (DEMS). DEMS experiments were carried out under room conditions in acid media, in an electrochemical cell directly coupled to the vacuum chamber of a mass spectrometer. The DEMS set-up was adapted in order to characterize GDEs [16]. In this way, the influence of the surface chemistry of carbon supports on the physicochemical and electrochemical properties of the electrodes for CO_2 reduction was studied. Formic acid ($m/z = 45$) was obtained as the main product on all the Fe/C electrodes, at potentials below −0.7 V vs. Ag/AgCl in 0.5 M H_2SO_4 at room temperature and atmospheric pressure (see Fig. 12). The formation of other products containing longer hydrocarbon chains was not discarded. This result is really noticeable, since bulk Fe electrodes produce mainly H_2 under the same conditions [90]. In addition, formic acid presents several applications for agriculture, chemical, textile and pharmaceutical industries, as well as for food technology. On the other hand, it was found that the carbon support and their surface chemistry presented a strong influence on the electrochemical reduction of CO_2, modifying the activity and selectivity of the process. In fact, oxygenated groups enhanced the catalytic activity toward CO_2 reduction (Fe/Vulcan NcTb0.5 and Fe/Vulcan NSTa0.5) in comparison to the electrode supported on the virgin material (Fe/Vulcan). However, the GDE treated in nitric acid during 2 h (Fe/Vulcan NcTb2) presented the lowest acid formic generation, which suggest that longer treatments with nitric acid destroy partially the structure of the support, decreasing its efficiency for CO_2 reduction [17].

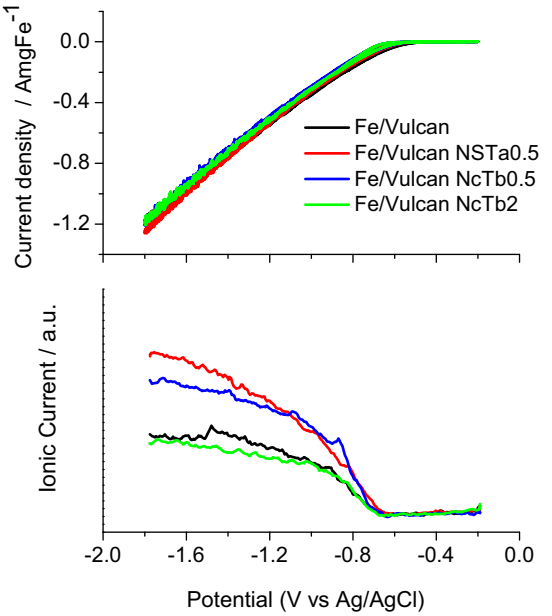

Fig. 12. (Colour online.) CVs (upper panel) and MSCV for formic acid (bottom panel, $m/z = 45$) with Fe/C catalysts in 0.5 M H_2SO_4. $\nu = 0.01$ V·s^{-1}.

4.2. Pd catalysts supported on nanostructured carbon materials

Pd is a hydrogen-storing material that may favour the adsorption of species derived from CO_2 reduction and their further transformation. However, the use of carbon-supported catalysts based on palladium has not been widely studied [111,112]. Recently, our research group has studied the electrochemical activity of Pd catalysts supported on different nanostructured carbon materials, including CNF, CNC, and OMC. Commercial carbon Vulcan XC-72R was also used for comparing results. Therefore, the influence of the carbon material on the physicochemical and electrochemical properties of the electrocatalysts was evaluated [18].

Carbon materials were prepared using different methods:

- methane decomposition for the synthesis of CNF;
- catalytic graphitization for CNC;
- nano-casting technique for OMC.

Pd electrocatalysts were prepared by the impregnation–reduction procedure with sodium borohydride. Appropriate amounts of metal precursor were employed to obtain a theoretical metal loading of 20 wt. % onto the different carbon materials [18]. The electrochemical properties of the catalysts were studied by cyclic voltammetry in $NaHCO_3$ 0.1 M. In addition, DEMS experiments were performed for registering simultaneously and "in situ" the formation of molecular hydrogen, which is produced during the reduction of CO_2.

Cyclic voltammetry studies in 0.1 M $NaHCO_3$ showed that CO_2 was effectively reduced at Pd/C electrocatalysts. As can be seen in Fig. 13 for the Pd/Vulcan catalyst, a peak around −1.0 V appeared in the current voltammogram during the cathodic scan, while two anodic signals were developed at 0.10 and 0.35 V. In addition, the production of H_2 decreased in the presence of CO_2. These results indicate

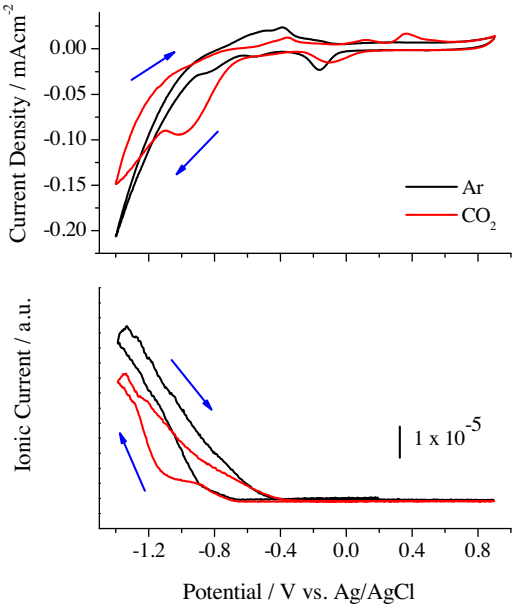

Fig. 13. (Colour online.) CVs (upper panel) and its corresponding MSCV for H_2 (bottom panel, $m/z = 2$) with Pd/Vulcan catalyst in 0.1 M $NaHCO_3$. $\nu = 0.01\ V{\cdot}s^{-1}$. Black curves: Ar saturated solution. Red curves: CO_2 saturated solution.

that at −1.0 V, CO_2 is reduced to other species $(CO_2)_{red}$, which are adsorbed at Pd/C surface and oxidized during the anodic excursion. According to the literature [93–95,100], these species are mainly CO_{ad}, although the presence of other adsorbates (such as $COOH_{ad}$, COH_{ad} or CHx) cannot be discarded. Similar results were obtained on the other electrocatalysts.

In order to verify the existence of adsorbed species, CO and "reduced CO_2" strippings were performed, by bubbling CO_2 at −0.5 V and −1.0 V, respectively [18]. Different oxidation charges were obtained from CO and "reduced CO_2" stripping $\left(Q_{CO_2,red}/Q_{CO}\right)$ for all the

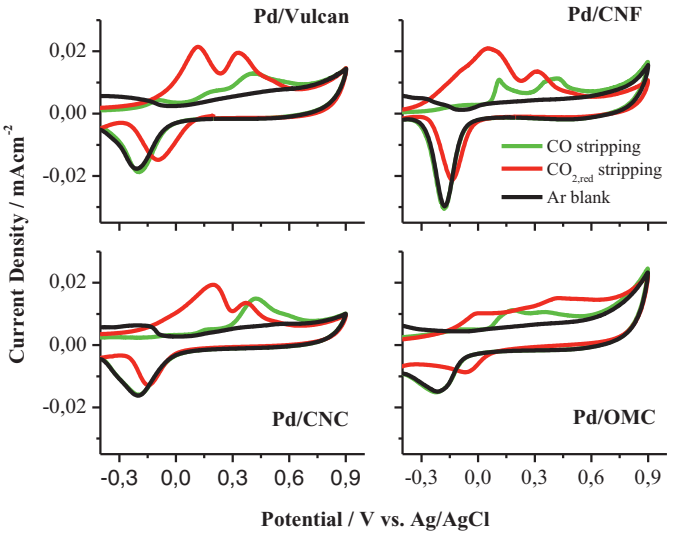

Fig. 14. (Colour online.) Comparison of CO and "reduced CO_2" stripping voltammograms for Pd/C catalysts in 0.1 M $NaHCO_3$. $\nu = 0.01\ V{\cdot}s^{-1}$.

samples, indicating that the adsorbed species were not only CO_{ad}, but also that other adsorbates could be formed ($COOH_{ad}$, COH_{ad}) (Fig. 14). In addition, different ratios $\left(Q_{CO_2,red}/Q_{CO}\right)$ were found for the electrocatalysts, probably due to a different product distribution. It could be explained from differences in the Pd–H_{ad} strength depending on the support, which might affect the catalytic activity towards CO_2 reduction.

5. Conclusions

Carbon has been used as a catalytic support due to its excellent properties. Nowadays, new nanostructure materials have been developed such as nanotubes, nanofibers, nanocoils, nanohorns and ordered mesoporous carbons, because they have a better pore structure, more uniform characteristics, a reduced number of impurities and a better electronic structure for different applications than conventional supports. The Fuel Conversion Research Group of ICB–CSIC has a long track record in the preparation and characterization of carbon materials. In this paper, three applications of carbon catalysts have been summarized: NO reduction over activated carbons in different shapes (powder, briquettes and monoliths), electrocatalysts for fuel cells synthetized over nanofibers, xerogels and ordered mesoporous carbons, electroreduction of CO_2 using Fe and Pd deposited onto carbon materials. The main conclusion of this work is that the properties of carbon supports have an enormous influence on the performance of carbon catalysts for all applications.

Acknowledgments

The authors gratefully acknowledge financial support given by Spanish MINECO (ENE2014-52518-C2-1-R). S. Pérez-Rodríguez and S. Ascaso acknowledge the "Gobierno de Aragón" and CSIC, respectively, for their postdoctoral grants. Furthermore, the authors wish to thank Dra. Elena Pastor and Dr. Gonzalo García (Universidad de La Laguna, Spain) for DEMS facilities and the discussion of the spectroelectrochemical results.

References

[1] C. Ampelli, S. Perathoner, G. Centi, Chin. J. Catal. 35 (2014) 783.
[2] D.S. Su, S. Perathoner, G. Centi, Chem. Rev. 113 (2013) 5782.
[3] P. Trogadas, T.F. Fuller, P. Strasser, Carbon 75 (2014) 5.
[4] L.-R. Radovic, C. Mora-Vilches, A.J.A. Salgado-Casanova, Chin. J. Catal. 35 (2014) 792.
[5] P. Serp, M. Corrias, P. Kalck, Appl. Catal., A: Gen. 253 (2003) 337.
[6] D. Sebastián, I. Suelves, R. Moliner, M.J. Lázaro, Carbon 48 (2010) 4421.
[7] D. Sebastián, I. Suelves, R. Moliner, M.J. Lázaro, A. Stassi, V. Baglio, A.S. Aricò, Appl. Catal., B 132–133 (2013) 22.
[8] D. Sebastián, I. Suelves, E. Pastor, R. Moliner, M.J. Lázaro, Appl. Catal., B 132–133 (2013) 13.
[9] V. Celorrio, L. Calvillo, M.V. Martínez-Huerta, R. Moliner, M.J. Lázaro, Energy Fuels 24 (2010) 3361.
[10] V. Celorrio, L. Calvillo, S. Pérez-Rodríguez, M.J. Lázaro, R. Moliner, Micropor. Mesopor. Mater. 142 (2011) 55–61.
[11] L. Calvillo, V. Celorrio, R. Moliner, P.L. Cabot, I. Esparbé, M.J. Lázaro, Micropor. Mesopor. Mater. 116 (2008) 292.
[12] M.J. Lázaro, L. Calvillo, E.G. Bordejé, R. Moliner, R. Juan, C.R. Ruiz, Micropor. Mesopor. Mater. 103 (2007) 158.
[13] C. Alegre, L. Calvillo, R. Moliner, J.A. González-Expósito, O. Guillén-Villafuerte, M.V.M. Huerta, E. Pastor, M.J. Lázaro, J. Power Sources 196 (2011) 4226.
[14] C. Alegre, M.E. Gálvez, E. Baquedano, E. Pastor, R. Moliner, M.J. Lázaro, Int. J. Hydrogen Energy 37 (2012) 7180.
[15] C. Alegre, M.E. Gálvez, R. Moliner, V. Baglio, A.S. Aricò, M.J. Lázaro, Appl. Catal., B 147 (2014) 947.
[16] S. Pérez-Rodríguez, M. Corengia, G. García, C.F. Zinola, M.J. Lázaro, E. Pastor, Int. J. Hydrogen Energy 37 (2012) 7141.
[17] S. Pérez-Rodríguez, G. García, L. Calvillo, V. Celorrio, E. Pastor, M.J. Lázaro, Int. J. Electrochem. 2011 (2011) 1–13.
[18] S. Pérez-Rodríguez, N. Rillo, M.J. Lázaro, E. Pastor, Appl. Catal., B 163 (2015) 83.
[19] D. Sebastián, C. Alegre, L. Calvillo, M. Pérez, R. Moliner, M.J. Lázaro, Int. J. Hydrogen Energy 39 (2014) 4109.
[20] M.E. Gálvez, M.J. Lázaro, R. Moliner, Catal. Today 102–103 (2005) 142.
[21] M.J. Lázaro, A. Boyano, M.E. Gálvez, M.T. Izquierdo, E. García-Bordejé, C. Ruiz, R. Juan, R. Moliner, Catal. Today 137 (2008) 215.
[22] M.J. Lázaro, M.E. Gálvez, C. Ruiz, R. Juan, R. Moliner, Appl. Catal., B: Environ. 68 (2006) 130.
[23] M.E. Gálvez, A. Boyano, M.J. Lázaro, R. Moliner, Chem. Eng. J. 144 (2008) 10.
[24] A. Boyano, M.E. Gálvez, M.J. Lázaro, R. Moliner, Carbon 44 (2006) 2399.
[25] M.J. Lázaro, A. Boyano, M.E. Gálvez, M.T. Izquierdo, R. Moliner, Catal. Today 119 (2007) 175.
[26] A. Boyano, M.E. Gálvez, R. Moliner, M.J. Lázaro, Catal. Today 137 (2008) 209.
[27] A. Boyano, M.E. Gálvez, R. Moliner, M.J. Lázaro, Fuel 87 (2008) 2058.
[28] M.E. Gálvez, A. Boyano, R. Moliner, M.J. Lázaro, J. Anal. Appl. Pyrolysis 88 (2010) 80.
[29] E. García-Bordejé, L. Calvillo, M.J. Lázaro, R. Moliner, Ind. Eng. Chem. Res. 43 (2004) 4073.
[30] E. García-Bordejé, L. Calvillo, M.J. Lázaro, R. Moliner, Appl. Catal., B: Environ. 50 (2004) 235.
[31] E. García-Bordejé, M.J. Lázaro, R. Moliner, P.M. Álvarez, V. Gómez-Serrano, J.L.G. Fierro, Carbon 44 (2006) 407.
[32] E. García-Bordejé, J.L. Pinilla, M.J. Lázaro, R. Moliner, Appl. Catal., B: Environ. 66 (2006) 281.
[33] M.J. Lázaro, D. Sebastián, I. Suelves, R. Moliner, J. Nanosci. Nanotechnol. 9 (2009) 4353.
[34] D. Sebastián, J.C. Calderón, J.A. González-Expósito, E. Pastor, M.V. Martínez-Huerta, I. Suelves, R. Moliner, M.J. Lázaro, Int. J. Hydrogen Energy 35 (2010) 9934.
[35] C. Alegre, M.E. Gálvez, R. Moliner, V. Baglio, A. Stassi, A.S. Aricò, M.J. Lázaro, Chem. Cat. Chem. 5 (2013) 3770.
[36] L. Calvillo, V. Celorrio, R. Moliner, A.B. García, I. Caméan, M.J. Lázaro, Electrochim. Acta 102 (2013) 19.
[37] L. Calvillo, V. Celorrio, R. Moliner, M.J. Lázaro, Mater. Chem. Phys. 127 (2011) 335.
[38] J.R.C. Salgado, F. Alcaide, G. Álvarez, L. Calvillo, M.J. Lázaro, E. Pastor, J. Power Sources 195 (2010) 4022.
[39] M.J. Lázaro, V. Celorrio, L. Calvillo, E. Pastor, R. Moliner, J. Power Sources 196 (2011) 4236.
[40] T. Suzuki, T. Kyotani, A. Tomita, Ind. Eng. Chem. Res. 33 (1994) 2840.
[41] M.J. Illán-Gómez, A. Linares-Solano, C. Salinas-Martínez De Lecea, J.M. Calo, Energy Fuels 7 (1993) 146.
[42] H. Teng, Y.T. Tu, Y.C. Lai, C.C. Lin, Carbon 39 (2001) 575.
[43] Z. Zhu, Z. Liu, S. Liu, H. Niu, Appl. Catal., B: Environ. 30 (2001) 267.
[44] T. Grzybek, J. Pasel, H. Papp, Phys. Chem. Chem. Phys. 1 (1999) 341.
[45] G. Marbán, A.B. Fuertes, Appl. Catal., B: Environ. 34 (2001) 55.
[46] G. Marbán, A.B. Fuertes, Appl. Catal., B: Environ. 34 (2001) 43.
[47] Z. Zhu, Z. Liu, S. Liu, H. Niu, Fuel 79 (2000) 651.
[48] T.M. Grant, C.J. King, Ind. Eng. Chem. Res. 29 (1990) 264.
[49] R.D. Vidic, C.H. Tessmer, L.J. Uranowski, Carbon 35 (1997) 1349.
[50] S.R. Richards, Fuel Process. Technol. 25 (1990) 89.
[51] B. Rubio, M.T. Izquierdo, E. Segura, Carbon 37 (1999) 1833.
[52] A. Amaya, N. Medero, N. Tancredi, H. Silva, C. Deiana, Bioresour. Technol. 98 (2007) 1635.
[53] J.I. Ozaki, Y. Nishiyama, P.J. Guy, G.J. Perry, D.J. Allardice, Fuel Process. Technol. 50 (1997) 57.
[54] R. Moliner, I. Suelves, M.J. Lázaro, O. Moreno, Int. J. Hydrogen Energy 30 (2005) 293.
[55] S. Srinivasan, B.B. Davé, K.A. Murugesamoorthi, A. Parthasarathy, A.J. Appleby, J. Blomen, M.N. Mugerwa (Eds.), Fuel Cell Systems, Plenum Press, New York, USA, 1993, pp. 37–72.
[56] W. Li, W. Zhou, H. Li, Z. Zhou, B. Zhou, G. Sun, Q. Xin, Electrochim. Acta 49 (2004) 1045.
[57] P. Costamagna, S. Srinivasan, J. Power Sources 102 (2001) 242.
[58] H.A. Gasteiger, N.M. Markovic, P.N. Ross Jr., J. Phys. Chem. 99 (1995) 8290.
[59] M. Watanabe, S. Motoo, J. Electroanal. Chem. 60 (1975) 267.
[60] E.M. Crabb, R. Marshall, D. Thompsett, J. Electrochem. Soc. 147 (2000) 4440.

[61] N.B. Grgur, N.M. Markovic, P.N. Ross, Electrochim. Acta 43 (1998) 3631.
[62] D.C. Papageorgopoulos, M. Keijzer, F.A. de Bruijn, Electrochim. Acta 48 (2002) 197.
[63] Z. Hou, B. Yi, H. Yu, Z. Lin, H. Zhang, J. Power Sources 123 (2003) 116.
[64] C.A. Bessel, K. Laubernds, N.M. Rodriguez, R.T.K. Baker, J. Phys. Chem. B 105 (2001) 1115.
[65] E.S. Steirgerwalt, G.A. Deluga, D.E. Cliffel, C.M. Lukehart, J. Phys. Chem. B 105 (2001) 8097.
[66] W. Li, C. Liang, J. Qiu, W. Zhou, H. Han, Z. Wei, G. Sun, Q. Xin, Carbon 40 (2002) 791.
[67] W. Chen, J.Y. Lee, Z. Liu, Mater. Lett. 58 (2004) 3166.
[68] Y.C. Liu, X.P. Qiu, Y.Q. Huang, W.T. Zhu, Carbon 40 (2002) 2375.
[69] R. Yang, X. Qiu, H. Zhang, J. Li, W. Zhu, Z. Wang, X. Huang, L. Chen, Carbon 43 (2005) 11.
[70] J. Marie, S. Berthon-Fabry, P. Achard, M. Chatenet, A. Pradourat, E. Chainet, J. Non-Cryst. Solids 350 (2004) 88.
[71] N. Job, J. Marie, S. Lambert, S. Berthon-Fabry, P. Achard, Energ. Convers. Manage 49 (2008) 2461.
[72] J. Ding, K.-Y. Chan, J. Ren, F.-S. Xiao, Electrochim. Acta 50 (2005) 3131.
[73] L. Calvillo, M.J. Lázaro, E.G. Bordejé, R. Moliner, P.L. Cabot, I. Esparbé, E. Pastor, J.J. Quintana, J. Power Sources 169 (2007) 59.
[74] N. Mahata, M.F.R. Pereira, F. Suárez-García, A. Martínez-Alonso, J.M.D. Tascón, J.L. Figueiredo, J. Colloid Interface Sci. 324 (2008) 150.
[75] R. Ryoo, S.H. Joo, S. Jun, T. Tsubakiyama, O. Terasaki, Stud. Surf. Sci. Catal. 135 (2001) 150.
[76] M. Tsuji, M. Kubokawa, R. Yano, N. Miyamae, T. Tsuji, M.S. Jun, S. Hong, S. Lim, S.H. Yoon, I. Mochida, Langmuir 23 (2007) 387.
[77] N.M. Rodríguez, J. Mater. Res. 8 (1993) 3233.
[78] T.V. Reshetenko, L.B. Avdeeva, Z.R. Ismagilov, A.L. Chuvilin, V.A. Ushakov, Appl. Catal., A 247 (2003) 51.
[79] A. Romero, A. Garrido, A. Nieto-Márquez, A.R. de la Osa, A. de Lucas, J.L. Valverde, Appl. Catal., A 319 (2007) 246.
[80] A.S. Aricò, V. Baglio, A. Di Blasi, E. Modica, G. Monforte, V. Antonucci, J. Electroanal. Chem. 576 (2005) 161.
[81] N. Job, R. Pirard, J. Marien, J.P. Pirard, Carbon 42 (2004) 3217.
[82] C. Arbizzani, S. Righi, F. Soavi, M. Mastragostino, Int. J. Hydrogen Energy 36 (2011) 5038.
[83] A. Taguchi, F. Schüth, Micropor. Mesopor. Mater. 77 (2005) 1.
[84] J. Li, X. Miao, Y. Hao, J. Zhao, X. Sun, L. Wang, J. Colloid Interf. Sci. 318 (2008) 309.
[85] Y. Xun, Z. Shu-Ping, X. Wei, C. Hong-You, D. Xiao-Dong, L. Xin-Mei, Y. Zi-Feng, J. Colloid Interf. Sci. 310 (2007) 83.
[86] J.-H. Zhou, J.-P. He, Y.-J. Ji, W.-J. Dang, X.-L. Liu, G.-W. Zhao, C.-X. Zhang, J.-S. Zhao, Q.-B. Fu, H.-P. Hu, Electrochim. Acta 52 (2007) 4691.
[87] R. Ryoo, S.H. Joo, M. Kruk, M. Jaroniec, Adv. Mater. 13 (2001) 677.
[88] M. Jitaru, D.A. Lowy, M. Toma, B.C. Toma, L. Oniciu, J. Appl. Electrochem. 27 (1997) 875.
[89] Y. Hori, H. Wakebe, T. Tsukamoto, O. Koga, Electrochim. Acta 39 (1994) 1833.
[90] Y. Hori, K. Kikuchi, S. Suzuki, Chem. Lett. 14 (1985) 1695.
[91] M. Gattrell, N. Gupta, A. Co, J. Electroanal. Chem. 594 (2006) 1.
[92] B. Beden, A. Bewick, M. Razaq, J. Weber, J. Electroanal. Chem. 139 (1982) 203.
[93] D. Kolbe, W. Vielstich, Electrochim. Acta 41 (1996) 2457.
[94] K. Ohkawa, K. Hashimoto, A. Fujishima, J. Electroanal. Chem. 345 (1993) 445.
[95] M. Azuma, K. Hashimoto, M. Watanabe, T. Sakata, J. Electroanal. Chem. 294 (1990) 299.
[96] H. De Jesús-Cardona, C. Del Moral, C.R. Cabrera, J. Electroanal. Chem. 513 (2001) 45.
[97] K. Hara, A. Kudo, T. Sakata, J. Electroanal. Chem. 391 (1995) 141.
[98] K. Hara, A. Kudo, T. Sakata, J. Electroanal. Chem. 386 (1995) 257.
[99] M. Azuma, K. Hashimoto, M. Hiramoto, M. Watanabe, T. Sakata, J. Electroanal. Chem. 260 (1989) 441.
[100] M. Azuma, K. Hashimoto, M. Hiramoto, M. Watanabe, T. Sakata, J. Electrochem. Soc. 137 (1990) 1772.
[101] S. Kaneco, N.H. Hiei, Y. Xing, H. Katsumata, H. Ohnishi, T. Suzuki, K. Ohta, Electrochim. Acta 48 (2002) 51.
[102] S. Kaneco, K. Iiba, K. Ohta, T. Mizuno, J. Solid State Electrochem. 3 (1999) 424.
[103] S. Kaneco, K. Iiba, H. Katsumata, T. Suzuki, K. Ohta, Electrochim. Acta 51 (2006) 4880.
[104] Y.B. Vassiliev, V.S. Bagotzky, O.A. Khazova, N.A. Mayorova, J. Electroanal. Chem. 189 (1985) 295.
[105] K. Ohta, M. Kawamoto, T. Mizuno, D.A. Lowy, J. Appl. Electrochem. 28 (1998) 717.
[106] P.A. Christensen, A. Hamnett, A.V.G. Muir, N.A. Freeman, J. Electroanal. Chem. 288 (1990) 197.
[107] M.N. Mahmood, D. Masheder, C.J. Harty, J. Appl. Electrochem. 17 (1987) 1159.
[108] R.L. Cook, R.C. MacDuff, A.F. Sammells, J. Electrochem. Soc. 137 (1990) 607.
[109] G. Centi, S. Perathoner, G. Winè, M. Gangeri, Green Chem. 9 (2007) 671.
[110] M. Gangeri, S. Perathoner, S. Caudo, G. Centi, J. Amadou, D. Bégin, C. Pham-Huu, M.J. Ledoux, J.P. Tessonnier, D.S. Su, R. Schlögl, Catal. Today 143 (2009) 57.
[111] N. Furuya, T. Yamazaki, M. Shibata, J. Electroanal. Chem. 431 (1997) 39.
[112] A. Bandi, M. Specht, T. Weimer, K. Schaber, Energy Convers. Manage 36 (1995) 899.